Original Article | Neuroimaging and Head & Neck

eISSN 2005-8330
https://doi.org/10.3348/kjr.2021.0477
Korean J Radiol 2022;23(4):446-454

Korean Journal of Radiology
KJR

Hyperoxia-Induced ΔR_1: MRI Biomarker of Histological Infarction in Acute Cerebral Stroke

Kye Jin Park[1*], Ji-Yeon Suh[2*], Changhoe Heo[2], Miyeon Kim[2], Jin Hee Baek[2], Jeong Kon Kim[1, 2]

[1]Department of Radiology and Research Institute of Radiology, University of Ulsan College of Medicine, Asan Medical Center, Seoul, Korea; [2]Asan Institute for Medical Sciences, University of Ulsan College of Medicine, Asan Medical Center, Seoul, Korea

Objective: To evaluate whether hyperoxia-induced ΔR_1 (hyper$O_2\Delta R_1$) can accurately identify histological infarction in an acute cerebral stroke model.

Materials and Methods: In 18 rats, MRI parameters, including hyper$O_2\Delta R_1$, apparent diffusion coefficient (ADC), cerebral blood flow and volume, and ^{18}F-fluorodeoxyglucose uptake on PET were measured 2.5, 4.5, and 6.5 hours after a 60-minutes occlusion of the right middle cerebral artery. Histological examination of the brain was performed immediately following the imaging studies. MRI and PET images were co-registered with digitized histological images. The ipsilateral hemisphere was divided into histological infarct (histological cell death), non-infarct ischemic (no cell death but ADC decrease), and non-ischemic (no cell death or ADC decrease) areas for comparisons of imaging parameters. The levels of hyper$O_2\Delta R_1$ and ADC were measured voxel-wise from the infarct core to the non-ischemic region. The correlation between areas of hyper$O_2\Delta R_1$-derived infarction and histological cell death was evaluated.

Results: Hyper$O_2\Delta R_1$ increased only in the infarct area ($p \leq 0.046$) compared to the other areas. ADC decreased stepwise from non-ischemic to infarct areas ($p = 0.002$ at all time points). The other parameters did not show consistent differences among the three areas across the three time points. Hyper$O_2\Delta R_1$ sharply declined from the core to the border of the infarct areas, whereas there was no change within the non-infarct areas. A hyper$O_2\Delta R_1$ value of 0.04 s^{-1} was considered the criterion to identify histological infarction. ADC increased gradually from the infarct core to the periphery, without a pronounced difference at the border between the infarct and non-infarct areas. Areas of hyper$O_2\Delta R_1$ higher than 0.04 s^{-1} on MRI were strongly positively correlated with histological cell death ($r = 0.862$; $p < 0.001$).

Conclusion: Hyper$O_2\Delta R_1$ may be used as an accurate and early (2.5 hours after onset) indicator of histological infarction in acute stroke.

Keywords: *MRI; Acute stroke; Infarction; Biomarker; Hyperoxia-induced ΔR_1*

INTRODUCTION

Currently, the early restoration of blood flow to non-infarct ischemic areas is the optimal treatment option to rescue brain tissue at risk of irreversible damage following acute stroke. However, many stroke patients experience neurological deterioration after successful vascular recanalization, even without hemorrhagic transformation [1]. These undesirable results imply that initial imaging examination may underestimate the area of irreversible damage; that is, infarction, or that progressive neuronal damage may occur even after the successful reperfusion of salvageable tissue. Therefore, an accurate imaging parameter is needed to measure the area of infarction to select adequate treatment and monitor treatment outcomes in acute stroke.

Although numerous imaging techniques have been used to identify infarction in acute stroke, they have limitations in accurately measuring the infarct area. The apparent diffusion coefficient (ADC) calculated from diffusion-

Received: June 25, 2021 **Revised:** November 9, 2021
Accepted: November 25, 2021
*These authors contributed equally to this work.
Corresponding author: Jeong Kon Kim, MD, PhD, Department of Radiology, University of Ulsan College of Medicine, Asan Medical Center, 88 Olympic-ro 43-gil, Songpa-gu, Seoul 05505, Korea.
• E-mail: kim.jeongkon@gmail.com

Korean Journal of Radiology
KJR

weighted imaging (DWI) is often renormalized during the aggravation of ischemic injury after recanalization, and perfusion-weighted imaging parameters do not indicate cell viability after vascular recanalization [2-4].

Hyperoxia-induced ΔR_1 (hyper$O_2\Delta R_1$) is a feasible MRI biomarker of tissue oxygen level [5-7]. Theoretically, this parameter is based on the oxygen-driven acceleration of longitudinal relaxation (quantified by increased R_1); thus, the difference in R_1 between hyperoxic and normoxic breathing (i.e., hyper$O_2\Delta R_1$) indicates the amount of oxygen accumulation during hyperoxic respiration and, therefore, demonstrates the status of oxygen delivery and consumption in tissue. Recently, Suh et al. [7] suggested that the tissue oxygenation status quantified by hyper$O_2\Delta R_1$ can be used to classify ischemic damage into exacerbating and devastated stages in the late phase (24 hours) following stroke onset. Based on this theoretical background, we hypothesized that hyper$O_2\Delta R_1$ may be useful in identifying irreversible ischemic damage, such as cell death, in acute stroke.

Of the various methods used to evaluate the severity of tissue impairment in acute stroke, morphological cell death by light microscopy is most frequently used to identify the area of infarction. Therefore, a meaningful correlation between morphological cell death and hyper$O_2\Delta R_1$ may indicate that this MRI-driven parameter can be used to identify irreversible ischemic damage in acute stroke. In this study, we evaluated whether hyper$O_2\Delta R_1$ can accurately identify histological infarction in an acute cerebral stroke model.

MATERIALS AND METHODS

All experimental protocols, including the animal care and experimental procedures in this study, were approved by the Institutional Animal Care and Use Committee of Asan Medical Center.

Transient Stroke Model

The right middle cerebral arteries (MCAs) of adult male Wistar rats (weight, 280–300 g) were occluded for 60 minutes using the intraluminal filament technique, as previously described [8]. The details are summarized in the Supplement.

MRI, ^{18}F-FDG PET, and Histology

MRI and PET were performed at three time points (2.5 hours, 4.5 hours, and 6.5 hours) following the initiation of transient stroke. The first image acquisition time of 2.5 hours was assigned for the stabilization of animal physiology, transfer, and fixation to the bed of imaging machines after surgery. Then, the time window between imaging experiments was arbitrarily assigned as 2 hours The histological examinations were performed immediately after imaging.

The MRI parameters were acquired using a 7T Bruker pre-clinical MRI scanner (PharmaScan 70/16, Brucker BioSpin GmbH), which included T2-weighted images (T2WIs), ADC images from DWI, hyper$O_2\Delta R_1$ from R_1 mapping, and cerebral blood flow (CBF) and volume (CBV) from dynamic susceptibility contrast imaging. The MRI acquisition parameters are listed in Table 1. ^{18}F-FDG PET was obtained before MRI using a nanoScanPET/MRI system (1T, Mediso), which provided the standard uptake value. Further details are provided in the Supplement.

Light microscopy histological examination was performed

Table 1. MRI Acquisition Parameters

	T2-Weighted Imaging	Diffusion-Weighted Imaging	Dynamic Susceptibility Contrast-Enhanced Imaging	R_1 Map
Sequence	Fast-spin echo sequence	Spin-echo EPI sequence	Gradient-echo EPI sequence	Relaxation-enhancement with variable repetition time sequence
TR/TE, ms	4000/33	3000/18.7	1000/16	TR = 600, 900, 1500, 2500, 4000, 7000; TE = 12.15
Other parameters	Rare factor = 8	b value (s/mm^2) = 0 and 800	Flip angle = 35°	Rare factor = 4
Field of view, mm	28 x 28	28 x 28	28 x 28	28 x 28
Matrix size	96 x 96	96 x 96	96 x 96	64 x 64
Slice number	16	16	16	16
Slice thickness, mm	1	1	1	1
Acquisition time	1 min 36 sec	3 min 36 sec	3 min	8 min 48 sec

EPI = echo planar imaging, TE = echo time, TR = repetition time

https://doi.org/10.3348/kjr.2021.0477

on the mid-coronal sections of the brain. Each brain section was stained with hematoxylin and eosin (H&E) and 0.25% cresyl violet for Nissl staining [9].

Based on the histologic findings and acceptable MRI and PET quality, this study included 18 rats with stroke, including six rats at each time point, which demonstrated histological infarction in more than one-third of the ipsilateral hemisphere.

Calculation of Hyper$O_2\Delta R_1$

To measure hyper$O_2\Delta R_1$, normoxic (20% oxygen) and hyperoxic (100% oxygen) gases were infused through a respiratory mask without mechanical ventilation. The gas flow was maintained at a constant rate (1 L/min at 1 atm) during the experiment. Hyperoxia-induced ΔR_1 was calculated according to the difference in R1 between hyperoxic and normoxic breathing. Further details are provided in the Supplement.

Co-Registration of Images to the Histological Map

Using T2WI as a reference frame, all parameter maps were co-registered and interpolated to achieve the same voxel geometry. For image-histology correlation, slices of MRI and PET images were selected and registered to the corresponding digitized histological map.

Image Analysis

The image analysis process is shown in Figure 1. The ipsilateral hemisphere was categorized into three areas based on the conjunction of the incorporated histological and ADC information. In this approach, the ADC value was used to identify the occurrence of ischemia, whereas histologic findings indicated irreversible severe damage (i.e., cell death). The histological findings were used to determine the viability of the given cells. Cells were identified as dead according to the presence of cell body shrinkage, darkly stained pyknotic nuclei, intensely stained red eosinophilic cytoplasm in H&E staining, and loss of Nissl substance in Nissl staining [10,11]. An ipsilateral-to-contralateral ratio of ADC < 0.95 indicated ischemic cell damage, as described previously [7]. These criteria of cell death or damage on ADC were then used to classify the ipsilateral hemisphere into three areas: histological infarct (cell death), non-infarct ischemic (cell damage without cell death), and non-ischemic (no cell death or damage). Regions-of-interest (ROIs) corresponding to the three areas were drawn on MRI and PET images co-registered to the histological map. The values of each imaging parameter were then compared among the three ROIs.

The delineation of the border between infarct and non-infarct areas requires setting a cutoff value to differentiate these areas. Accordingly, we performed a voxel-scaled line study to continuously measure hyper$O_2\Delta R_1$ and ADC. In each rat, we drew a line from the infarct center to the periventricular non-ischemic region on images co-registered with the histologic map. Every line was drawn

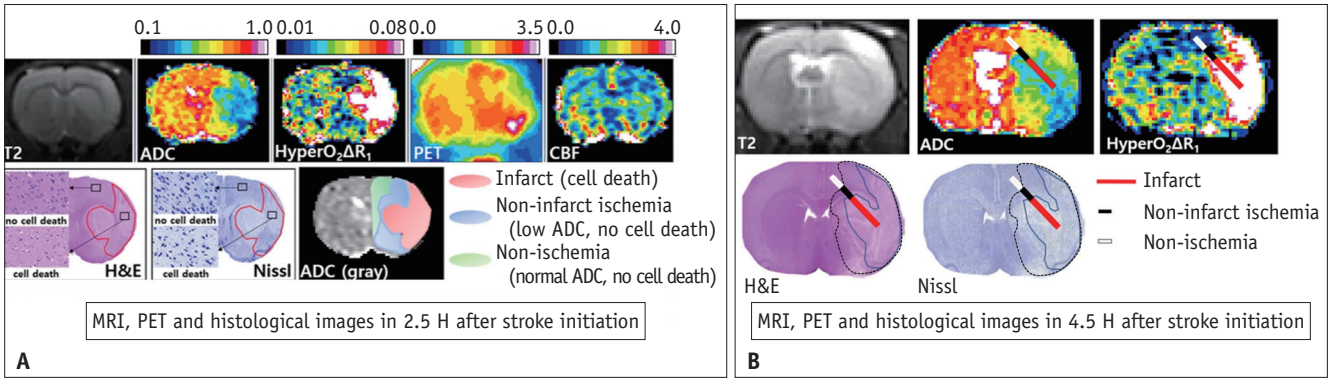

Fig. 1. Image analysis.

A. The ipsilateral hemisphere was categorized into infarct, ischemic, and non-ischemic areas based on histological findings and ADC values. Areas with histologic findings indicated cell death, including cell body shrinkage, darkly stained pyknotic nuclei in H&E stain (x 20), and a loss of Nissl substance in Nissl staining (x 20), were considered infarct. The imaging parameters were then compared in these three areas. **B.** Voxel-wise line analysis of hyper$O_2\Delta R_1$ and ADC values from the center of the infarct (outlined by blue in H&E stain [x 20] and Nissl stain [x 20], representing histologic cell death) to the non-ischemic area. Here, areas with ipsilateral-to-contralateral ratios of ADC < 0.95 are outlined by a black dashed line, and the area between the blue (i.e., cell death) and black dashed lines define non-infarct ischemia. On MRI, a line is drawn from the infarct center to the periventricular non-ischemic region on images co-registered to the histologic map. Every line is drawn to cross the three areas with identical proportions: 60% of the total length of each line crossed the infarct area, 20% crossed the non-infarct ischemic area, and the remaining 20% crossed the non-ischemic area. ADC = apparent diffusion coefficient, CBF = cerebral blood flow, FDG = fluorodeoxyglucose, H = hours, H&E = hematoxylin and eosin, hyper$O_2\Delta R_1$ = hyperoxia-induced ΔR_1

https://doi.org/10.3348/kjr.2021.0477

Korean Journal of Radiology
KJR

to proportionally identically cross the three areas: 60% of the total length of each line crossed the infarct area, 20% crossed the non-infarct ischemic area, and the remaining 20% crossed the non-ischemic area. This approach allowed the integrated analysis of the changes in hyper$O_2\Delta R_1$ and ADC from the infarct core to the non-ischemic area in all rats. In addition, the correlations between the image parameters measured on the lines were also analyzed.

Finally, to validate whether the hyper$O_2\Delta R_1$ could be used to locate the infarct area, we assessed the spatial correlation between hyper$O_2\Delta R_1$ and histological features. The area of infarction indicated by hyper$O_2\Delta R_1$ was measured and its ratio in the area of the ipsilateral hemisphere was calculated. The area ratio of cell death lesions in the ipsilateral hemisphere was also estimated on the histological map.

Statistical Analysis

The Friedman test was used to compare each value across the three areas. In cases of statistical significance, Wilcoxon signed-rank tests were performed for *post-hoc* analysis. Spearman correlation was used to evaluate the correlations between the areas of hyper$O_2\Delta R_1$-derived infarction and histological cell death. Statistical significance was set at $p < 0.05$.

RESULTS

MRI and PET Parameters according to Histology at Each Time Point

Figure 2 and Table 2 show the values of imaging parameters measured in the histological infarct, non-infarct ischemic, and non-ischemic areas at the three time points (2.5, 4.5, and 6.5 hours). Compared to the other parameters, hyper$O_2\Delta R_1$ showed a distinctive pattern in terms of discrimination of the infarct area, with increased values occurring exclusively in the infarct area ($p \leq 0.046$) compared to the other areas (Supplementary Table 1). This pattern was consistently observed at all three time points. In contrast, the ADC values demonstrated a pattern of stepwise decrease from the non-ischemic to infarct areas at all time points ($p = 0.002$ at all time points).

^{18}F-FDG uptake, CBF, and CBV did not show consistent differences among the three areas across the three time points (Supplementary Fig. 1). ^{18}F-FDG uptake was higher in the infarct area than in the other areas at 2.5 hours,

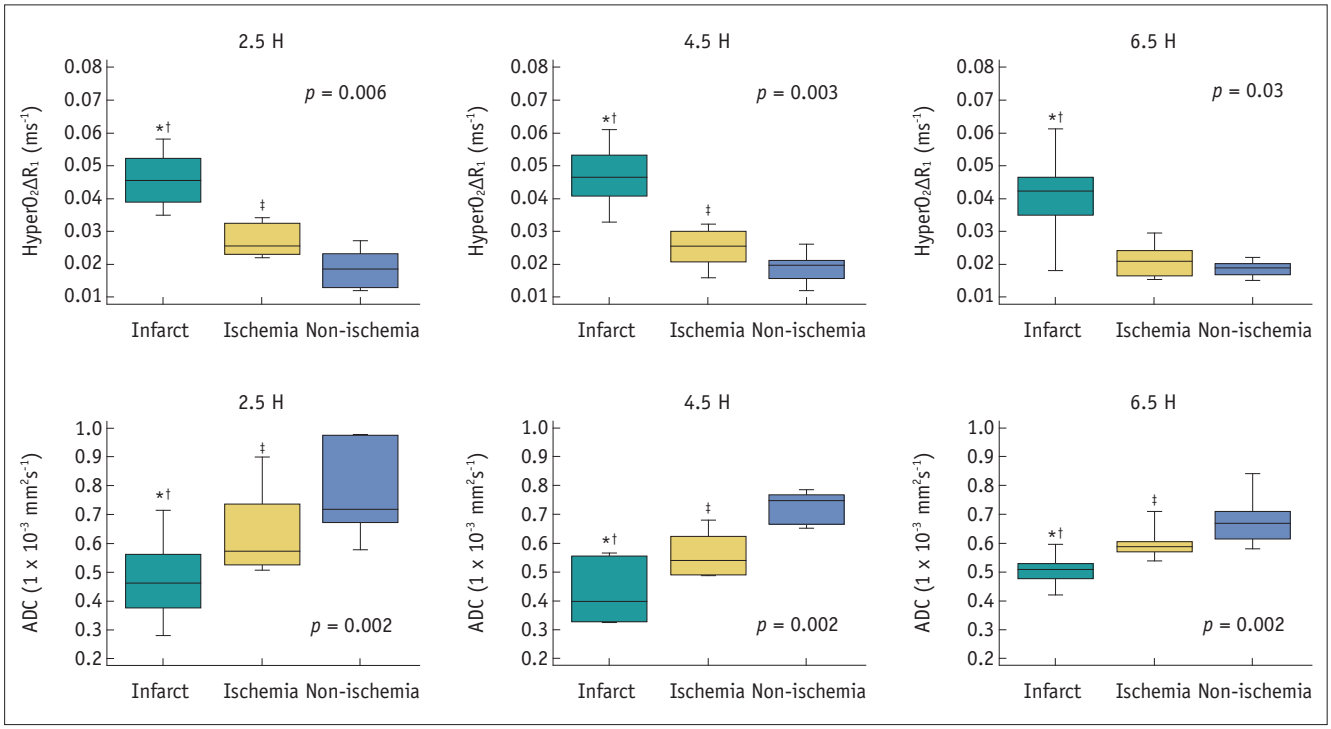

Fig. 2. Comparisons of hyper$O_2\Delta R_1$ and ADC in infarct, ischemic, and non-ischemic areas. Hyper$O_2\Delta R_1$ increases only in the infarct area at all three time points. In contrast, the ADC values demonstrate a pattern of stepwise decrease from the non-ischemic to infarct areas at all time points. *Statistically significant difference between infarct and ischemia, †Statistically significant difference between infarct and non-ischemia, ‡Statistically significant difference between ischemia and non-ischemia. ADC = apparent diffusion coefficient, hyper$O_2\Delta R_1$ = hyperoxia-induced ΔR_1

https://doi.org/10.3348/kjr.2021.0477

Table 2. MRI and PET Parameters in Infarct, Ischemia, and Non-Ischemia Areas

	Hyper$O_2\Delta R_1$ (10^{-2} ms)	ADC (10^{-4} mm^2 s^{-1})	^{18}F-FDG Uptake	CBF (mL/g/min)	CBV (ms^{-1})
2.5 H					
Infarct	4.6 ± 0.9	4.8 ± 1.5	2.9 ± 0.6	0.9 ± 0.2	34 ± 8
Ischemia	2.7 ± 0.5	6.4 ± 1.5	2.3 ± 0.3	1.3 ± 0.4	44 ± 11
Non-ischemia	1.9 ± 0.6	7.7 ± 1.7	2.0 ± 0.3	1.6 ± 0.7	45 ± 11
4.5 H					
Infarct	4.7 ± 1.0	4.3 ± 1.1	1.7 ± 0.3	1.3 ± 0.5	43 ± 18
Ischemia	2.5 ± 0.6	5.6 ± 0.8	2.0 ± 0.2	1.4 ± 0.5	44 ± 13
Non-ischemia	1.6 ± 0.5	7.3 ± 0.5	2.0 ± 0.2	1.5 ± 0.5	44 ± 14
6.5 H					
Infarct	4.1 ± 1.4	5.1 ± 0.7	1.8 ± 0.5	2.2 ± 1.4	64 ± 35
Ischemia	2.1 ± 0.5	6.1 ± 0.8	2.0 ± 0.2	2.4 ± 1.1	53 ± 25
Non-ischemia	1.9 ± 0.2	6.8 ± 0.9	2.0 ± 0.4	2.3 ± 1.1	65 ± 25

Data are presented as mean ± standard deviation. ADC = apparent diffusion coefficient, CBF = cerebral blood flow, CBV = cerebral blood volume, FDG = fluorodeoxyglucose, Hyper$O_2\Delta R_1$ = hyperoxia-induced ΔR_1

but not at 4.5 and 6.5 hours. Likewise, differences in CBF and CBV were observed only at 2.5 hours (p = 0.009 and 0.011, respectively), when those values were lower in the infarct area compared to the other areas. The CBF value was lower in the infarct area at 4.5 hours (p = 0.042) compared to the non-ischemic area, although the difference was not significant compared to the ischemic area. The lack of significant between-area differences in the CBF and CBV levels at 4.5 and 6.5 hours indicated that the blood supply was restored and evenly distributed across all areas after the transient occlusion of the MCA. Given the inconsistent patterns or differences across the time points, the parameters of ^{18}F-FDG, CBF, and CBV were inadequate for use as reproducible biomarkers for assessment of the degree of ischemic injury.

Voxel-Wise Line Analysis of Hyper$O_2\Delta R_1$ and ADC

Based on the ROI experiments, hyper$O_2\Delta R_1$ and ADC were chosen as imaging parameters for further investigation to discriminate areas of irreversible and reversible ischemic damage.

hHyper$O_2\Delta R_1$ and ADC showed different distributions in voxels arranged on lines drawn from the infarct core to the non-ischemic area (Fig. 1B). Hyper$O_2\Delta R_1$ showed a sharp decline in the voxel values moving from the core to the border of the infarct areas, whereas there was no change within the non-infarct areas (Fig. 3A). Hyper$O_2\Delta R_1$ was > 0.04 s^{-1} in most of the voxels included in the infarct area and < 0.04 s^{-1} in the voxels in the non-infarct areas. We observed no notable difference in hyper$O_2\Delta R_1$ between the non-infarct ischemic and non-ischemic areas. In contrast, ADC showed a pattern of gradual increase from the infarct core to the periphery without a pronounced difference at the border between the infarct and non-infarct ischemic areas (Fig. 3B). Thus, it was difficult to assign a clear ADC cutoff value to clearly define the border between the infarct and non-infarct areas.

The correlation between hyper$O_2\Delta R_1$ and ADC showed a dichotomized pattern, as shown in Figure 3C. In the voxels with hyper$O_2\Delta R_1$ < 0.04 s^{-1}, most of which were identified in the non-infarcted and non-ischemic areas, hyper$O_2\Delta R_1$ and ADC showed a strong negative correlation. In contrast, the voxels with hyper$O_2\Delta R_1$ > 0.04 s^{-1}, which were observed mostly in the infarct area, showed plateaued ADC values, regardless of the hyper$O_2\Delta R_1$ values. This dichotomized distribution was consistently observed at all time points after stroke onset. The negative correlation between the two parameters demonstrated that cell edema gradually progressed because of continual energy failure, while the plateaued correlation reflects the fact that brain tissue with hyper$O_2\Delta R_1$ > 0.04 > s^{-1} was maintained under the highest degree of cellular edema or restricted cytoplasmic movement. Therefore, we presume that a hyper$O_2\Delta R_1$ of 0.04 s^{-1} could indicate complete membrane failure of ischemic cells in acute stroke.

Correlation between Hyper$O_2\Delta R_1$ Area and Histological Infarct Area

Areas of hyper$O_2\Delta R_1$ > 0.04 s^{-1} were strongly positively correlated with those of histological cell death (r =

https://doi.org/10.3348/kjr.2021.0477

Korean Journal of Radiology
KJR

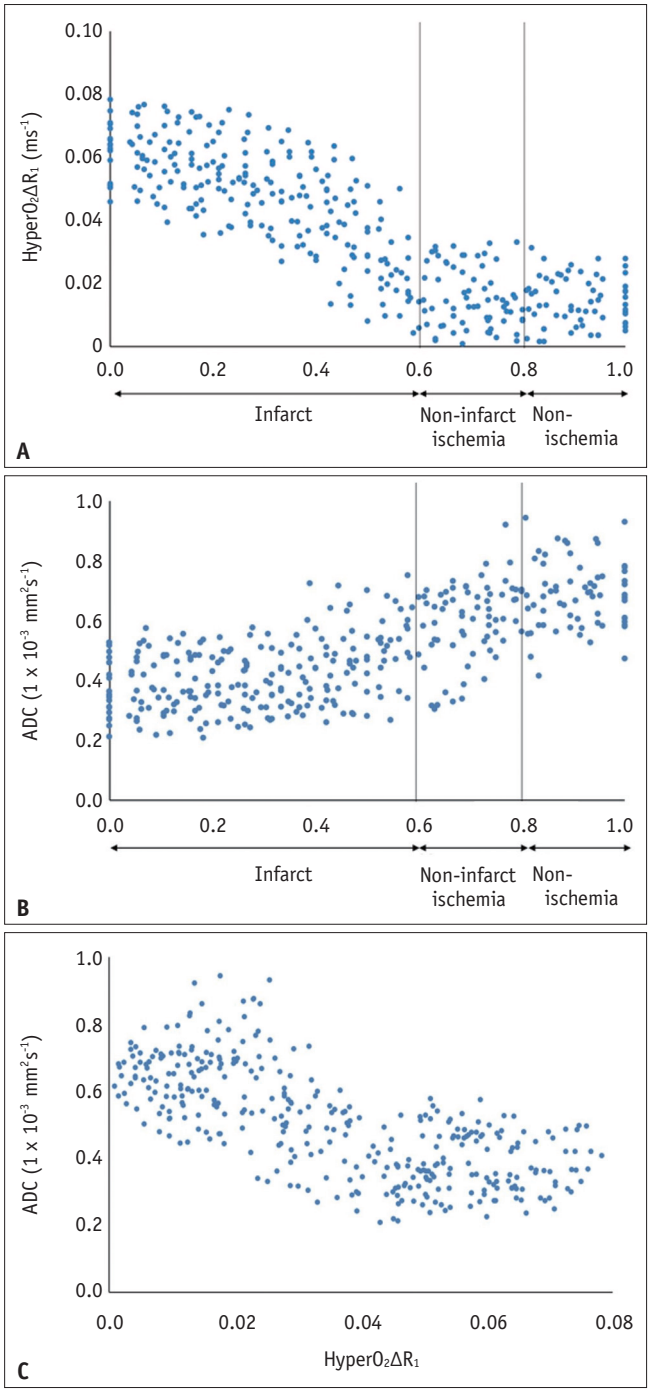

Fig. 3. Voxel-wise line analysis of hyper$O_2\Delta R_1$ and ADC values from the center of the infarct to the non-ischemic area.
A. Scatterplot demonstrating a clear transition in hyper$O_2\Delta R_1$ values at the border of the infarct core and non-infarct ischemia area at a cutoff of 0.4 s^{-1}. **B.** Monotonic increase in ADC values from the infarct core to the non-ischemic area, with no clear boundary between areas. **C.** Scatterplot demonstrating the negative correlation between hyper$O_2\Delta R_1$ and ADC values below the hyper$O_2\Delta R_1$ cutoff of 0.04 s^{-1}, and a plateaued distribution of ADC values above 0.04 s^{-1}. ADC = apparent diffusion coefficient, hyper$O_2\Delta R_1$ = hyperoxia-induced ΔR_1

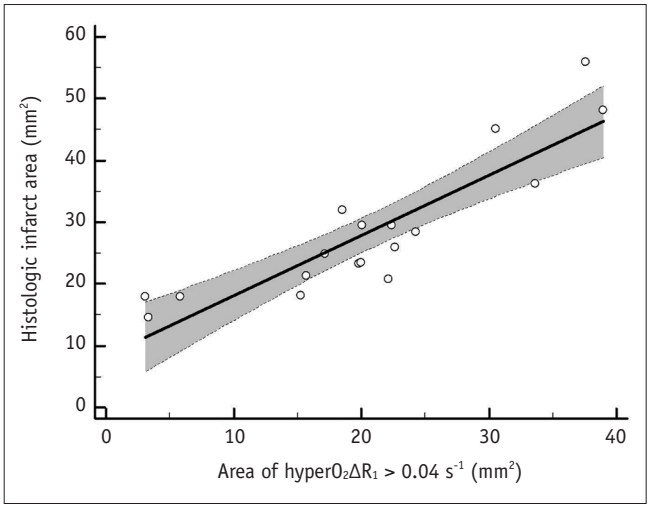

Fig. 4. Strong positive correlation between the histologically defined infarct area and the area with hyper$O_2\Delta R_1$ greater than 0.04 s^{-1} (r = 0.862). hyper$O_2\Delta R_1$ = hyperoxia-induced ΔR_1

0.862; p < 0.001) (Fig. 4). On visual inspection, the areas of hyper$O_2\Delta R_1$ > 0.04 s^{-1} spatially corresponded with the histologically determined areas of cell death. Thus, hyper$O_2\Delta R_1$ was an accurate indicator of the location of the area of histological infarct.

DISCUSSION

In our study, hyper$O_2\Delta R_1$ values increased at various time points only in the areas with histological cell death and differed notably at the borders between cell death and other areas. These results demonstrated that hyper$O_2\Delta R_1$ can consistently identify the cell death area in any time window of acute stroke. Our findings subsequently showed that areas with hyper$O_2\Delta R_1$ values > 0.04 s^{-1} were very similar to areas showing cell death on histological analysis. The results of the cross-sectional study validated that a hyper$O_2\Delta R_1$ value > 0.04 s^{-1} is a reliable indicator of histological cell death; that is, irreversible ischemic damage, in stroke. A longitudinal study is needed to track the fate of an area with hyper$O_2\Delta R_1$ values > 0.04 s^{-1} in each rat to more accurately demonstrate the ability of this criterion to differentiate irreversible from reversible ischemic damage.

The hyper$O_2\Delta R_1$ value is determined by the balance between oxygen delivery and consumption in the tissue. In cells under hypoxic damage in acute stroke, cellular oxygen utilization for energy production remains hypoactivated, even after the blood supply is restored. This condition

https://doi.org/10.3348/kjr.2021.0477

leads to an accumulation of unconsumed oxygen during hyperoxic respiration, which consequently increases hyper$O_2\Delta R_1$ (i.e., the difference in R_1 between hyperoxic and normoxic respiration). Therefore, increased hyper$O_2\Delta R_1$ in the transient ischemic brain is an MRI phenotype reflecting impaired oxygen metabolism.

As mitochondria consume oxygen for energy production, hyper$O_2\Delta R_1$ quantification of unconsumed oxygen indicates the degree of mitochondrial dysfunction. Various harmful processes in mitochondria, such as altered biogenetics, disorganized structural architecture, and aberrant biochemical dynamics, play a pivotal role in neuronal death in stroke [12]. Mitochondrial damage leads not only to the depletion of energy production but also to an overproduction of reactive oxygen species. In addition to the collapse of electrophysiological homeostasis due to a lack of energy, reactive oxygen species induce pathological processes that cause neuronal death, such as caspase activation, the release of inflammatory mediators, and oxidative damage to the cell [13,14]. Therefore, our criteria of a hyper$O_2\Delta R_1 > 0.04\ s^{-1}$, which showed a close correlation between histological cell death and failure of renormalization, may indicate irreversible neuronal death triggered by mitochondrial dysfunction in stroke.

T2WI, DWI, and perfusion imaging have been widely used in both preclinical and clinical trials to measure areas with reversible or irreversible damage [15-17]. However, the origins of the signals on T2WI (water content), DWI (diffusivity of water protons), and perfusion imaging (delivery of contrast material) do not provide information on cell viability, and accurate cutoff values to distinguish reversible and irreversible damage have not been identified for these MRI methods. Furthermore, perfusion imaging has a significant limitation in terms of reliability, as perfusion-related parameters vary according to the calculation algorithm and the location used to extract the arterial input function [18,19].

In response to these limitations, we attempted to systemically validate the utility of hyper$O_2\Delta R_1$ for identifying regions with irreversible damage. We found that 1) measurements at various time points showed the reliability of hyper$O_2\Delta R_1$ for identifying irreversible damage, 2) voxel-wise analysis allowed the establishment of criteria to delineate the border between infarct and non-infarct areas, and 3) the areas with histological cell death and hyper$O_2\Delta R_1 > 0.04\ s^{-1}$ were similar. These findings validate the efficacy and reliability of a hyper$O_2\Delta R_1$ value $> 0.04\ s^{-1}$ to estimate areas with irreversible damage.

The results of the present study demonstrated that the ADC may not be an adequate marker to identify irreversible ischemic damage; moreover, because of the gradual progression from non-ischemia to infarct, it was difficult to assign a cutoff ADC value to delineate the infarct area. Despite these limitations, as the ADC is particularly useful for assessing ischemic damage; thus, we recommend the combined implementation of ADC and hyper$O_2\Delta R_1$ (decreased ADC and hyper$O_2\Delta R_1 < 0.04\ s^{-1}$) to provide more accurate and reliable information for identifying non-infarct ischemia. Using these criteria, improvement from non-infarct ischemia to non-ischemia can be identified, as was observed for the spontaneous improvement shown in this study.

Several potential concerns and challenges must be addressed to apply hyper$O_2\Delta R_1$ in clinical settings. First, application of administration of 100% O_2 for several minutes may raise a concern regarding oxygen toxicity. Actually, hyperbaric oxygen therapy in longer than 60 minutes has risks of harmful effects [20,21]. However, the use of hyper$O_2\Delta R_1$ only for several minutes is unlikely to produce any harmful effects. Nevertheless, to completely remove such a risk, a maximum measurement time to guarantee safety must be established. The inevitable extension of examination time because of our recommended acquisition of multiple parameters (hyper$O_2\Delta R_1$ in conjunction with ADC or CBF) is another important point of concern, as it is critical to minimize the scanning time in patients with acute stroke. Thus, we propose the use of ultrafast scanning techniques. Using the Look-Locker technique, R_1 maps of the entire human brain can be acquired within 2 minutes, with a spatial resolution of 1.1 x 1.1 x 4 mm^3 [22]. Another faster MRI sequence is the ultrafast low-angle RARE sequence, which has a temporal resolution that allows the measurement of R_1 in the mouse brain within 6 seconds [23]. Moreover, as the R_1 relaxation time can be influenced by the magnetic field strength, the hyper$O_2\Delta R_1 > 0.04\ s^{-1}$ determined in our study on a 9.4T MRI system cannot be generally applied to 1.5T or 3T MRI systems. For example, the cutoff of $0.05\ s^{-1}$ used in the previous study was determined under a 4.7T MRI system; thus, further refinement is needed for application in the clinical setting.

Several methods are used for the histological characterization of acute stroke, including 2,3,5-Triphenyltetrazolium chloride (TTC), H&E, Nissl, and caspase staining. TTC is one of the most widely used methods. This study used methods requiring glass slides,

https://doi.org/10.3348/kjr.2021.0477

Korean Journal of Radiology
KJR

including H&E and Nissl staining, because they allow easier and more orthogonal photographic images that are required for co-registration with MRI images. Moreover, H&E and Nissl staining provide a wider time window for histological analysis compared to TTC [10].

In summary, the results of our study showed that MRI-driven hyper$O_2\Delta R_1$ above 0.04 s^{-1} delineated areas with histological cell death 2.5 hours after stroke onset. In conjunction with other traditional MRI parameters, the use of hyper$O_2\Delta R_1$ to identify areas with irreversible ischemic damage could help in determining adequate treatment and monitoring treatment effects in acute stroke.

Supplement

The Supplement is available with this article at https://doi.org/10.3348/kjr.2021.0477.

Availability of Data and Material

The datasets generated or analyzed during the study are available from the corresponding author on reasonable request.

Conflicts of Interest

The authors have no potential conflicts of interest to disclose.

Author Contributions

Conceptualization: all authors. Data curation: all authors. Formal analysis: all authors. Funding acquisition: all authors. Investigation: all authors. Methodology: all authors. Project administration: all authors. Resources: all authors. Software: all authors. Supervision: all authors. Validation: all authors. Visualization: all authors. Writing—original draft: all authors. Writing—review & editing: all authors.

ORCID iDs

Kye Jin Park
https://orcid.org/0000-0001-8428-436X
Ji-Yeon Suh
https://orcid.org/0000-0002-1177-2992
Changhoe Heo
https://orcid.org/0000-0002-5580-6568
Miyeon Kim
https://orcid.org/0000-0002-8797-2296
Jin Hee Baek
https://orcid.org/0000-0001-9343-4964
Jeong Kon Kim
https://orcid.org/0000-0001-5987-443X

Funding Statement

This work was supported by the Basic Science Research Program through the National Research Foundation of Korea (NRF) funded by the Ministry of Education, Science and Technology (2017R1A2B3007567) and through the Korea Health Industry Development Institute (KHIDI) funded by the Ministry of Health & Welfare, Republic of Korea (HI14C1090).

REFERENCES

1. Zhang YB, Su YY, He YB, Liu YF, Liu G, Fan LL. Early neurological deterioration after recanalization treatment in patients with acute ischemic stroke: a retrospective study. *Chin Med J (Engl)* 2018;131:137-143
2. Li F, Liu KF, Silva MD, Meng X, Gerriets T, Helmer KG, et al. Acute postischemic renormalization of the apparent diffusion coefficient of water is not associated with reversal of astrocytic swelling and neuronal shrinkage in rats. *AJNR Am J Neuroradiol* 2002;23:180-188
3. Leigh R, Knutsson L, Zhou J, van Zijl PC. Imaging the physiological evolution of the ischemic penumbra in acute ischemic stroke. *J Cereb Blood Flow Metab* 2018;38:1500-1516
4. Shen Q, Du F, Huang S, Duong TQ. Spatiotemporal characteristics of postischemic hyperperfusion with respect to changes in T1, T2, diffusion, angiography, and blood-brain barrier permeability. *J Cereb Blood Flow Metab* 2011;31:2076-2085
5. Colliez F, Safronova MM, Magat J, Joudiou N, Peeters AP, Jordan BF, et al. Oxygen mapping within healthy and acutely infarcted brain tissue in humans using the nmr relaxation of lipids: a proof-of-concept translational study. *PLoS One* 2015;10:e0135248
6. O'Connor JP, Boult JK, Jamin Y, Babur M, Finegan KG, Williams KJ, et al. Oxygen-enhanced mri accurately identifies, quantifies, and maps tumor hypoxia in preclinical cancer models. *Cancer Res* 2016;76:787-795
7. Suh JY, Cho G, Song Y, Woo DC, Choi YS, Ryu EK, et al. Hyperoxia-Induced ΔR1. *Stroke* 2018;49:3012-3019
8. Longa EZ, Weinstein PR, Carlson S, Cummins R. Reversible middle cerebral artery occlusion without craniectomy in rats. *Stroke* 1989;20:84-91
9. Popp A, Jaenisch N, Witte OW, Frahm C. Identification of ischemic regions in a rat model of stroke. *PLoS One* 2009;4:e4764
10. Zille M, Farr TD, Przesdzing I, Müller J, Sommer C, Dirnagl U, et al. Visualizing cell death in experimental focal cerebral ischemia: promises, problems, and perspectives. *J Cereb Blood Flow Metab* 2012;32:213-231

11. Li H, Zhang N, Lin HY, Yu Y, Cai QY, Ma L, et al. Histological, cellular and behavioral assessments of stroke outcomes after photothrombosis-induced ischemia in adult mice. *BMC Neurosci* 2014;15:58
12. Liu F, Lu J, Manaenko A, Tang J, Hu Q. Mitochondria in ischemic stroke: new insight and implications. *Aging Dis* 2018;9:924-937
13. Yang JL, Mukda S, Chen SD. Diverse roles of mitochondria in ischemic stroke. *Redox Biol* 2018;16:263-275
14. Crack PJ, Taylor JM. Reactive oxygen species and the modulation of stroke. *Free Radic Biol Med* 2005;38:1433-1444
15. Singhal AB, Benner T, Roccatagliata L, Koroshetz WJ, Schaefer PW, Lo EH, et al. A pilot study of normobaric oxygen therapy in acute ischemic stroke. *Stroke* 2005;36:797-802
16. Wintermark M, Albers GW, Broderick JP, Demchuk AM, Fiebach JB, Fiehler J, et al. Acute stroke imaging research roadmap II. *Stroke* 2013;44:2628-2639
17. Butcher KS, Parsons MW, Davis S, Donnan G. PWI/DWI mismatch: better definition required. *Stroke* 2003;34:e215-e216
18. Kidwell CS. MRI biomarkers in acute ischemic stroke: a conceptual framework and historical analysis. *Stroke* 2013;44:570-578
19. Bateman M, Slater LA, Leslie-Mazwi T, Simonsen CZ, Stuckey S, Chandra RV. Diffusion and perfusion mr imaging in acute stroke: clinical utility and potential limitations for treatment selection. *Top Magn Reson Imaging* 2017;26:77-82
20. Ding Z, Tong WC, Lu XX, Peng HP. Hyperbaric oxygen therapy in acute ischemic stroke: a review. *Interv Neurol* 2014;2:201-211
21. Rusyniak DE, Kirk MA, May JD, Kao LW, Brizendine EJ, Welch JL, et al. Hyperbaric oxygen therapy in acute ischemic stroke: results of the hyperbaric oxygen in acute ischemic stroke trial pilot study. *Stroke* 2003;34:571-574
22. Jiang K, Zhu Y, Jia S, Wu Y, Liu X, Chung YC. Fast T1 mapping of the brain at high field using Look-Locker and fast imaging. *Magn Reson Imaging* 2017;36:49-55
23. Pastor G, Jiménez-González M, Plaza-García S, Beraza M, Reese T. Fast T1 and T2 mapping methods: the zoomed U-FLARE sequence compared with EPI and snapshot-FLASH for abdominal imaging at 11.7 tesla. *MAGMA* 2017;30:299-307

https://doi.org/10.3348/kjr.2021.0477